Hybrid Spectral Polarization and Amplitude Coding implemented with Specified Orthogonal Ternary Code in Optical CDMA Network

Jen-Fa Huang
Department of Electrical Engineering, and Institute of Electro-Optical Science /Engineering
e-mail huajf@ee.ncku.edu.tw
(NSC94-2215-E-006-049)

Yao-Tang Chang
Department of Electrical Engineering and Institute of Electro- Engineering
e-mail n2891116@ccmail.ncku.edu.tw

Abstract

An improved hybrid spectral polarization and amplitude coding (hybrid SPC/SAC) scheme is implemented with specified orthogonal ternary sequence. In the previous spectral polarization (SPC) scheme, the entire wavelength is assigned as vertical or horizontal state of polarization (SOP), respectively. In current study, we assign positive (+), negative (-), and nothing chip (0) value on individual wavelengths allocation to realize the specified orthogonal ternary sequence which transformed from original bipolar Walsh-Hadamard matrix. The motivation of this manner is to reduce the phase induced intensity noise (PIIN) resulting from the wavelengths collision on photo-detector. It is shown that wavelength collision can be decreased and PIIN is also reduced at photo-detector. Neglecting the effects of shot noise and thermal noise, and considering only phase-induced intensity-noise with a degree of polarization setting of $\boldsymbol{P} = 0$ for the ideal case, the bit error rate versus the number of simultaneous active users is improved by 41.5% compared to the previous spectral polarization coding scheme for a 10^{-9} error probability.

Key index： Optical Code-Division Multiple-Access (OCDMA) Hybrid Spectral Polarization and amplitude Coding (Hybrid SPC/SAC), Fiber Bragg Gratings (FBGs), Polarization beam splitter (PBS), Phase-Induced Intensity Noise (PIIN).

1. Introduction

The SAC-OCDMA system was proposed as a means of increasing the maximum permissible number of simultaneous active users by decreasing the codeword length and eliminating the MAI effect [1-5]. Traditional spectral-amplitude coding (SAC) schemes can be classified as being either conventional unipolar SACs or complementary unipolar SACs. A conventional unipolar SAC transmits optical pulses only on data bit one, and sends nothing on data bit of zero. However, a complementary unipolar SAC transmits the specific codeword on data bit one and its complementary codeword on data bit of zero.

A crucial SAC problem is that of the phase-induced intensity-noise (PIIN) arising when mixed incoherent light fields are incident upon a photo-detector. The increased PIIN limits the maximum number of simultaneous active users [6-8]. A fundamental approach to overcome the PIIN problem is to reduce the number of wavelength collisions in the photo-detector.

In order to improve the spectral efficiency and overcome the phase induced intensity noise (PIIN), Huang at et al. configured the complementary bipolar spectral amplitude coding (SPC) scheme [8]. In the previous SPC scheme, fiber-Bragg-gratings (FBGs) are adopted as wavelength selectors for specified wavelength allocation according to the signature address code. Meanwhile, polarization beam splitters (PBSs) are employed to form two orthogonal SOPs from an un-polarized laser source. In addition, Walsh-Hadamard code is employed as the signature address code to allocate the specified wavelength an individual vertical or horizontal SOP. Hence, the complementary bipolar spectral amplitude coding (SPC) can be implemented by incorporating with polarization coding scheme.

In current study, a hybrid spectral polarization and amplitude coding (hybrid SPC/SAC) scheme is presented to improve the previous SPC scheme. Here, the specified orthogonal ternary sequence is transformed from original Walsh-Hadamard matrix. We assign positive (+), negative (-), and nothing chip (0) value on wavelengths allocation. Following the previous done work [8], a positive chip value (+1) is assigned to the vertical SOP, while a negative chip value (-1) is assigned to the horizontal SOP. The major difference is nothing chip (0) value is used to reduce wavelength collision such that the PIIN is also reduced at photo-detector.

The remainder of this paper is organized as follows. In the section 2, the specified orthogonal ternary matrix, which transformed from the Walsh-Hadamard codes matrix, is presented. Section 3 describes the proposed encoder and decoder (codecs) of hybrid SPC/SAC scheme based on specified orthogonal ternary code. The illustrative example is demonstrated in multiple access interference (MAI) in section 4. The Section 5 evaluates the system performance in terms of the BER and the maximum number of permissible simultaneous active users. The simulation results are compared with those of the unipolar and bipolar SAC approach to evaluate the performance improvement. Finally, Section 6 provides some concluding remarks.

2. The Specified Orthogonal Ternary Sequence Matrix

The original Walsh-Hadamard matrix form is expressed as is expressed as

$$\boldsymbol{H}_1 = \begin{bmatrix} \mathbf{1} & \mathbf{1} \\ \mathbf{1} & \mathbf{-1} \end{bmatrix} \text{ and } \boldsymbol{H}_\mathrm{n} = \begin{bmatrix} \boldsymbol{H}_{\mathrm{n}\text{-}1} & \boldsymbol{H}_{\mathrm{n}\text{-}1} \\ \boldsymbol{H}_{\mathrm{n}\text{-}1} & \text{-}\boldsymbol{H}_{\mathrm{n}\text{-}1} \end{bmatrix}$$

where n=2, 3, 4… (1)

Here, the row of Walsh-Hadamard matrix $\boldsymbol{H}$ is assigned as the codeword. Based on the original Hadamard matrix $\boldsymbol{H}$ and employing trying-and-error simulation, the proposed specified orthogonal ternary matrix **ST** is simple formulated by the adding or subtracting operation from the specified row pair of $\boldsymbol{H}$. Hence, the specific pairing rule is written as:

while $i \le N/4$

$$\mathbf{c}_{2i-1} = \left(\mathbf{h}_i + \mathbf{h}_{N-2(i-1)}\right) \times \frac{1}{2}$$

$$\mathbf{c}_{2i} = \left(\mathbf{h}_i - \mathbf{h}_{N-2(i-1)}\right) \times \frac{1}{2}$$

and

while $i > N/4$

$$\mathbf{c}_{2i-1} = \left(\mathbf{h}_i + \mathbf{h}_{2i-1}\right) \times \frac{1}{2}$$

$$\mathbf{c}_{2i} = \left(\mathbf{h}_i - \mathbf{h}_{2i-1}\right) \times \frac{1}{2} \qquad (2)$$

where x is multiple operator and $\mathbf{c}_{2i-1}$, $\mathbf{c}_{2i}$, $i = 1, 2, \ldots, N/2$, where $N=2^j$, j=3, 5, 7……, are the specified orthogonal ternary code and $\mathbf{h}_i$ denotes the i-th row of NxN Walsh-Hadamard matrix. Here, since the row of specified orthogonal ternary **ST** matrix is changed from the linear transformation (i.e., the adding or subtracting operation), the **ST** matrix is characterized by quasi-orthogonal property and suitable for spectral amplitude coding (SAC) scheme. Furthermore, the codeword (row) of **ST** matrix exist the least wavelength pulse to prevent the wavelength collision. Following the simple principle on Eq. (2), the simple example of 8x8 proposed specified orthogonal ternary **ST** is described as follows. We select the first and the eighth rows of Hadamard matrix $\boldsymbol{H}$ as a pair to produce the first and the second row of specified orthogonal ternary sequence matrix **ST** via adding/subtracting operation. For convenience, the above mentioned process is called that (row 1 + row 8, row 1 - row 8)$_{\boldsymbol{H}}$ transfer to (row 1, row 2)$_{\mathbf{ST}}$. Note that the subscript of $\boldsymbol{H}$ and **ST** denotes Walsh-Hadamard and specified orthogonal ternary sequence matrix, respectively. Similarly, (row 2 + row 6, row 2 - row 6)$_{\boldsymbol{H}}$ transfer to (row 3, row 4)$_{\mathbf{ST}}$, (row 3 + row 5, row3 - row5)$_{\boldsymbol{H}}$ transfer to (row 5, row 6)$_{\mathbf{ST}}$, and (row 4 + row 7, row 4 – row 7)$_{\boldsymbol{H}}$ transfer to (row 7, row 8)$_{\mathbf{ST}}$. Thus, the specified orthogonal ternary sequence matrix **ST** is produced as Fig. 1.

$$\begin{bmatrix} + & + & + & + & + & + & + & + \\ + & - & + & - & + & - & + & - \\ + & + & - & - & + & + & - & - \\ + & - & - & + & + & - & - & + \\ + & + & + & + & - & - & - & - \\ + & - & + & - & - & + & - & + \\ + & + & - & - & - & - & + & + \\ + & - & - & + & - & + & + & - \end{bmatrix}_{\boldsymbol{H}} \xrightarrow{\textbf{Transfer}} \begin{bmatrix} + & 0 & 0 & + & 0 & + & + & 0 \\ 0 & + & + & 0 & + & 0 & 0 & + \\ + & - & + & - & 0 & 0 & 0 & 0 \\ 0 & 0 & 0 & 0 & + & - & + & - \\ + & + & 0 & 0 & 0 & 0 & - & - \\ 0 & 0 & - & - & + & + & 0 & 0 \\ + & 0 & - & 0 & 0 & - & 0 & + \\ 0 & - & 0 & + & + & 0 & - & 0 \end{bmatrix}_{\mathbf{ST}}$$

Fig. 1. The created processing of specified orthogonal ternary matrix.

The orthogonal specified orthogonal ternary matrix **ST** can be decomposed into $\left(\mathbf{C}^{(1)}, \mathbf{C}^{(2)}\right)$ and expressed as Eq. (3). Hence, the k-th row of $\left(\mathbf{C}^{(1)}, \mathbf{C}^{(2)}\right)$ is denoted as $\left(\mathbf{c}_\mathbf{k}^{(1)}, \mathbf{c}_\mathbf{k}^{(2)}\right)$ and assigned as the signature code of the k-th user's as the signature code.

$$\mathbf{ST} = \begin{bmatrix} 1 & 0 & 0 & 1 & 0 & 1 & 1 & 0 \\ 0 & 1 & 1 & 0 & 1 & 0 & 0 & 1 \\ 1 & -1 & 1 & -1 & 0 & 0 & 0 & 0 \\ 0 & 0 & 0 & 0 & 1 & -1 & 1 & -1 \\ 1 & 1 & 0 & 0 & 0 & 0 & -1 & -1 \\ 0 & 0 & -1 & -1 & 1 & 1 & 0 & 0 \\ 1 & 0 & -1 & 0 & 0 & -1 & 0 & 1 \\ 0 & -1 & 0 & 1 & 1 & 0 & -1 & 0 \end{bmatrix}$$

$$= \begin{bmatrix} 1 & 0 & 0 & 1 & 0 & 1 & 1 & 0 \\ 0 & 1 & 1 & 0 & 1 & 0 & 0 & 1 \\ 1 & 0 & 1 & 0 & 0 & 0 & 0 & 0 \\ 0 & 0 & 0 & 0 & 1 & 0 & 1 & 0 \\ 1 & 1 & 0 & 0 & 0 & 0 & 0 & 0 \\ 0 & 0 & 0 & 0 & 1 & 1 & 0 & 0 \\ 1 & 0 & 0 & 0 & 0 & 0 & 0 & 1 \\ 0 & 0 & 0 & 1 & 1 & 0 & 0 & 0 \end{bmatrix} - \begin{bmatrix} 0 & 0 & 0 & 0 & 0 & 0 & 0 & 0 \\ 0 & 0 & 0 & 0 & 0 & 0 & 0 & 0 \\ 0 & 1 & 0 & 1 & 0 & 0 & 0 & 0 \\ 0 & 0 & 0 & 0 & 0 & 1 & 0 & 1 \\ 0 & 0 & 0 & 0 & 0 & 0 & 1 & 1 \\ 0 & 0 & 1 & 1 & 0 & 0 & 0 & 0 \\ 0 & 0 & 1 & 0 & 0 & 1 & 0 & 0 \\ 0 & 1 & 0 & 0 & 0 & 0 & 1 & 0 \end{bmatrix}$$

$$= \mathbf{C}^{(1)} - \mathbf{C}^{(2)} \qquad (3)$$

Based on Eq. (3), it implies that the $\mathbf{C}^{(1)} - \mathbf{C}^{(2)}$ expresses for the users with transmitting data bit of '1', where positive chip value (+) is referred to as vertical SOP assigning to this wavelength, and negative chip value (-) is referred to as horizontal SOP assigning to this wavelength. Also, the null chip value implies nothing wavelength is assigned for specified ternary. Conversely, while the data bit of '0' is transmitted, the $\mathbf{C}^{(1)} - \mathbf{C}^{(2)}$ sequence is assigned. It is obvious that vertical and horizontal SOP for wavelengths allocation is exchanged. Mapping the specified orthogonal ternary sequence matrix to wavelengths allocation characterized with two orthogonal polarization states, the codeword set is created and shown as Table 1 (a) and (b) for data bit '1' and ‘0’, respectively. The sign ‘+’ and ‘-’corresponds to orthogonal polarization states that is vertical and horizontal SOP and $\mathbf{c}_k$ denotes the k-th row of $\mathbf{C}$.

Table 1.
Specified orthogonal ternary codeword set for (a) data bit of ‘1’ and (b) data bit of ‘0’.
(a)

codeword	λ_1	λ_2	λ_3	λ_4	λ_5	λ_6	λ_7	λ_8
$\mathbf{c}_1$	+	0	0	+	0	+	+	0
$\mathbf{c}_2$	0	+	+	0	+	0	0	+
$\mathbf{c}_3$	+	-	+	-	0	0	0	0
$\mathbf{c}_4$	0	0	0	0	+	-	+	-
$\mathbf{c}_5$	+	+	0	0	0	0	-	-
$\mathbf{c}_6$	0	0	-	-	+	+	0	0
$\mathbf{c}_7$	+	0	-	0	0	-	0	+
$\mathbf{c}_8$	0	-	0	+	+	0	-	0

(b)

codeword	λ_1	λ_2	λ_3	λ_4	λ_5	λ_6	λ_7	λ_8
$\mathbf{c}_1$	-	0	0	-	0	-	-	0
$\mathbf{c}_2$	0	-	-	0	-	0	0	-
$\mathbf{c}_3$	-	+	-	+	0	0	0	0
$\mathbf{c}_4$	0	0	0	0	-	+	-	+
$\mathbf{c}_5$	-	-	0	0	0	0	+	+
$\mathbf{c}_6$	0	0	+	+	-	-	0	0
$\mathbf{c}_7$	-	0	+	0	0	+	0	-
$\mathbf{c}_8$	0	+	0	-	-	0	+	0

3. The Hybrid SPC/SAC Encoder and Decoder

As shown in Fig. 2, in order to implement bipolar complementary coding, the proposed scheme employs a symmetric pair of hybrid SPC/SAC encoders linked by a switch whose operation is controlled by the logic state of the transmitted data bits. When a data bit of “1” is transmitted, the switch directs the unpolarized light to the upper branch of the encoder. Conversely, the unpolarized light is switched to the lower branch when a data bit of “0” is transmitted. Note that c_6^1 and c_6^2 written with the FBGs have the same wavelength but orthogonal SOPs in the upper and lower branches.

When a data bit of “1” is transmitted, the detailed mechanisms and configuration of one branch of the present original encoder are shown in Fig. 2. The encoding procedure is the same as the previous SPC scheme. However, $\left(\mathbf{C},\overline{\mathbf{C}}\right)$ is replaced by $\left(\mathbf{C}^{(1)},\mathbf{C}^{(2)}\right)$ coding pattern [9]. For the user # 6 example, The reflected wavelengths with inverse SOPs are combined by the PBS and output at port 4 in the form of an encoded light wave (0, 0, λ_{3H}, λ_{4H}, λ_{5V}, λ_{6V}, 0, 0).

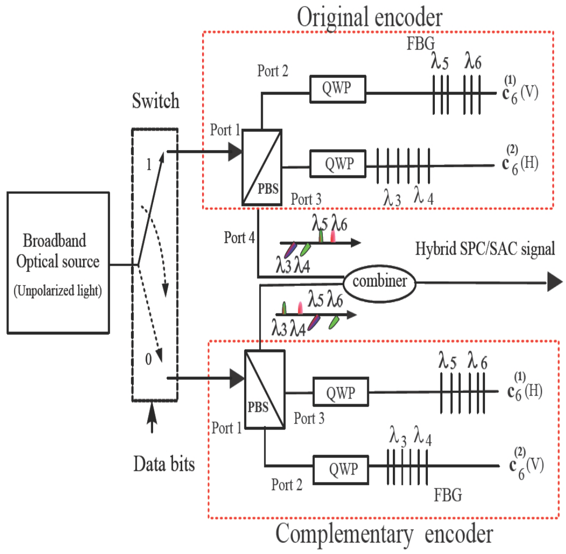

Fig. 2. Proposed encoder for user #6 with specified ternary code (0 0 - - + + 0 0). H : horizontal SOP, V : vertical SOP, QWP : quarter-wave plate.

The spectral light wave signals $\boldsymbol{R}$ encoded by each hybrid SPC/SAC encoder are summed and then transmitted to the network receivers in the system by a $\boldsymbol{K}$ x $\boldsymbol{K}$ star coupler. The summed signal spectrum for all the simultaneous active users, $\boldsymbol{K}$, is composed of vertical and horizontal states of polarization and is given by:

$$\boldsymbol{R} = \boldsymbol{R}_{\mathbf{V}} + \boldsymbol{R}_{\mathbf{H}} \tag{4}$$

where $$\boldsymbol{R}_{\mathbf{V}} = \sum_{k=1}^{K} \mathrm{b}_k \mathbf{c}_k^{(1)} + \left(1-\mathrm{b}_k\right) \mathbf{c}_k^{(2)}$$

and $$\boldsymbol{R}_{\mathbf{H}} = \sum_{k=1}^{K} \mathrm{b}_k \mathbf{c}_k^{(2)} + \left(1-\mathrm{b}_k\right) \mathbf{c}_k^{(1)}$$

In the current correlation filter process, the decoding procedure comprises five steps, as shown in Fig. 3. The symbols ① to ⑤ denote the sequence in which the steps of the correlation procedure are performed. The polarization states are indicated as **(H)** and **(V)** in each correlation procedure, respectively.

Similarly, the encoding procedure is the same as the previous SPC scheme. However, $\left(\mathbf{C},\overline{\mathbf{C}}\right)$ is replaced by $\left(\mathbf{C}^{(1)},\mathbf{C}^{(2)}\right)$ coding pattern [9].

However, the major difference compared the previous SPC decoder is shown as Fig. 3. Note that the no assigned FBG are used to filter out the wavelength transmitted from the QWP2. For user #6 example, the proposed ternary code of user #6 is assigned the absent wavelength of λ_1, λ_2, λ_7 and λ_8 (i.e., neither vertical nor horizontal state of polarization). Hence, the additional null wavelength assigned decoder is needed to reflect wavelength of λ_3, λ_4, λ_5 and λ_6 again. It mean that the null chip value "0" (i.e., λ_1, λ_2, λ_7 and λ_8**)** can be filter out to prevent impinging in photo-detector. Subsequently, the desired wavelengths impinge in the differential photo-detector one (PD1) and differential photo-detector two (PD2).

Hence, after the fifth step of the decoding procedure, and rearranging terms, the j-th detected power units are yielded as:

$$\left(\boldsymbol{R}_{\mathbf{V}}\cdot \mathbf{c}_j^{(1)}+\boldsymbol{R}_{\mathbf{H}}\cdot \mathbf{c}_j^{(2)}\right)-\left(\boldsymbol{R}_{\mathbf{V}}\cdot \mathbf{c}_j^{(2)}+\boldsymbol{R}_{\mathbf{H}}\cdot \mathbf{c}_j^{(1)}\right) \quad (5)$$
$$=\left(\boldsymbol{R}_{\mathbf{V}}+\boldsymbol{R}_{\mathbf{H}}\right)\cdot\left(\mathbf{c}_j^{(1)}-\mathbf{c}_j^{(2)}\right)=\boldsymbol{R}\cdot\left(\mathbf{c}_j^{(1)}-\mathbf{c}_j^{(2)}\right)$$

where $c_6^{(1)}$ and $c_6^{(2)}$ is the j-th user's coding pattern with vertical and horizontal SOP in the spectral domain, respectively. It can be seen that Eq. (5) performs a correlation function of $\boldsymbol{R}$ and $\mathbf{c}_j^{(1)}-\mathbf{c}_j^{(2)}$. It implies the proposed decoder perform the complementary ternary function and different from previous complementary bipolar function.

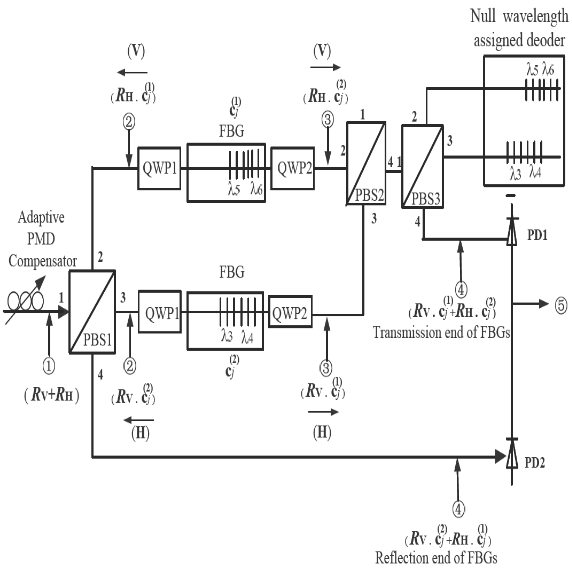

Fig. 3. Proposed decoder for user #6 with specified ternary code (0 0 - - + + 0 0).

4 The Example illustration of Hybrid SPC/SAC Coding

The detected power units by balanced detection (PD1-PD2) is written as

$$\mathbf{PD}1-\mathbf{PD}2=\sum_{k=1}^{K}\left(2b_k-1\right)\left(\mathbf{c}_k^{(1)}\cdot\mathbf{c}_j^{(1)}+\mathbf{c}_k^{(2)}\cdot\mathbf{c}_j^{(2)}\right)$$
$$-\sum_{k=1}^{K}\left(2b_k-1\right)\left(\mathbf{c}_k^{(2)}\cdot\mathbf{c}_j^{(1)}+\mathbf{c}_k^{(1)}\cdot\mathbf{c}_j^{(2)}\right) \quad (6)$$

The in-phase correlation for the k-th and the j-th users is $\mathbf{c}_k^{(1)}\cdot\mathbf{c}_j^{(1)}+\mathbf{c}_k^{(2)}\cdot\mathbf{c}_j^{(2)}$ and $\mathbf{c}_k^{(1)}\cdot\mathbf{c}_j^{(2)}+\mathbf{c}_k^{(2)}\cdot\mathbf{c}_j^{(1)}$ at PD1 and PD2, for $N=2^i$, i=3, 5, 7……, which are written as

$$\mathbf{c}_k^{(1)}\cdot\mathbf{c}_j^{(1)}+\mathbf{c}_k^{(2)}\cdot\mathbf{c}_j^{(2)}=\sum_{i=1}^{N}c_k^{(1)}(i)c_j^{(1)}(i)+c_k^{(2)}(i)c_j^{(2)}(i)$$
$$=\begin{cases}N/2 & \text{for } k=j\\ 0 & \text{for } k=j+1,\ k<j\\ N/8 & \text{otherwise}\end{cases} \quad (7a)$$

$$\mathbf{c}_k^{(1)}\cdot\mathbf{c}_j^{(2)}+\mathbf{c}_k^{(2)}\cdot\mathbf{c}_j^{(1)}=\sum_{i=1}^{N}c_k^{(1)}(i)c_j^{(2)}(i)+c_k^{(2)}(i)c_j^{(1)}(i)$$
$$=\begin{cases}0 & \text{for } k=j\\ 0 & \text{for } k=j+1,\ k<j\\ N/8 & \text{otherwise}\end{cases} \quad (7b)$$

Seen in Fig. 4, the simulation results verify the multiple access interference (MAI) is completely cancellation based on Eq. (7). Where x-axis denotes the simultaneous active users and y-axis is the detected power unit at decoder #8. It is assumed each user is transmitted the data bit of '1'.

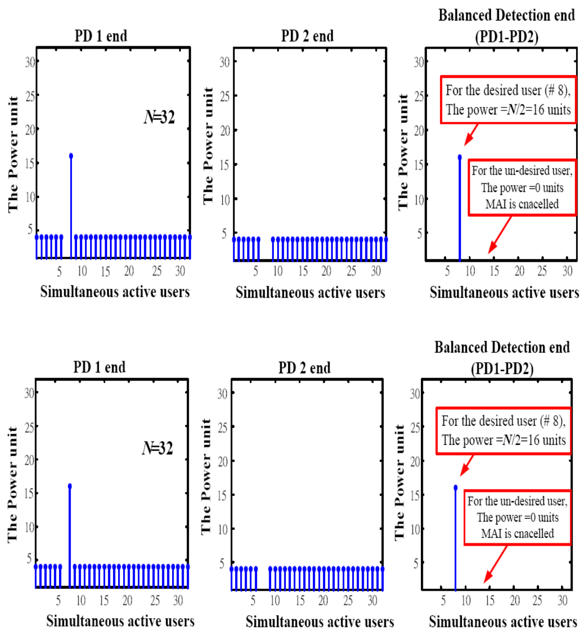

Fig. 4. The 8-th desired decoder power detection for user capacity of (a) N=32 and (b) N=128 when users is transmitted the data bit of '1'.

Seen in Figure 4, the matched codec for decoder #8 with transmitting data bit '1', the PD1 and PD2 detect $N/2$ and zero power units, respectively. The unmatched codec for decoder #8, the PD1 and PD2 detected $N/4$ power units equally, and balanced detection is $N/2$ power units for matched codec. The MAI is eliminated.

Table 2
Received signal for each user transmitting with specified ternary sequence.

	Data bit	Transmitted optical signal: Vertical SOP	λ_1	λ_2	λ_3	λ_4	λ_5	λ_6	λ_7	λ_8	Horizontal SOP	λ_1	λ_2	λ_3	λ_4	λ_5	λ_6	λ_7	λ_8
User #1	1	$C_1^{(1)}$	1	0	0	1	0	1	1	0	$C_1^{(2)}$	0	0	0	0	0	0	0	0
User #2	0	$C_2^{(2)}$	0	0	0	0	0	0	0	0	$C_2^{(1)}$	0	1	1	0	1	0	0	1
User #3	1	$C_3^{(1)}$	1	0	1	0	0	0	0	0	$C_3^{(2)}$	0	1	0	1	0	0	0	0
User #4	1	$C_4^{(1)}$	0	0	0	0	1	0	1	0	$C_4^{(2)}$	0	0	0	0	0	1	0	1
User #5	1	$C_5^{(1)}$	1	1	0	0	0	0	0	0	$C_5^{(2)}$	0	0	0	0	0	0	1	1
User #6	0	$C_6^{(2)}$	0	0	1	1	0	0	0	0	$C_6^{(1)}$	0	0	0	0	1	1	0	0
User #7	0	$C_7^{(2)}$	0	0	1	0	0	1	0	0	$C_7^{(1)}$	1	0	0	0	0	0	0	1
User #8	0	$C_8^{(2)}$	0	1	0	0	0	0	1	0	$C_8^{(1)}$	0	0	0	1	1	0	0	0
Received signal R		R_V	3	2	3	2	1	2	3	0	R_H	1	2	1	2	3	2	1	4

Table 2 show that the transmitting signature code for user #1~8 with data bit '1' or '0'. For the user with transmitting data bit '1', the transmitted signal is $\mathbf{c}_k^{(1)}$ for R_V and $\mathbf{c}_k^{(2)}$ for R_H. Conversely, the transmitted signal is $\mathbf{c}_k^{(1)}$ for R_H and $\mathbf{c}_k^{(2)}$ for R_V with transmitting data bit '0'. The simultaneous active users are 8 and the received signal spectrum is R. PBS split the received signal into RV and RH, and the reflected wavelengths according to the $\mathbf{c}_k^{(1)}$ and $\mathbf{c}_k^{(2)}$ for $\boldsymbol{R}_V$ and $\boldsymbol{R}_H$, respectively. The reflected wavelengths are launched into PD1 and PD2.

For the matched codec (ex. User #4) with transmitting data bit '1', the detected power units are $\boldsymbol{R}_\mathbf{H}\cdot\mathbf{c}_j^{(1)}$ + $\boldsymbol{R}_\mathbf{V}\cdot\mathbf{c}_j^{(2)}$ = 10 at PD1, and $\boldsymbol{R}_\mathbf{H}\cdot\mathbf{c}_j^{(2)}$ + $\boldsymbol{R}_\mathbf{V}\cdot\mathbf{c}_j^{1}$ = 6 at PD2. After the differential detection, the detected power units are 4, and the data bit '1' is recovery for user #4. Similarly, for the matched codec (ex. User #6), the detected power units are $\boldsymbol{R}_\mathbf{H}\cdot\mathbf{c}_j^{(1)}$ + $\boldsymbol{R}_\mathbf{V}\cdot\mathbf{c}_j^{(2)}$ = 6 at PD1, and $\boldsymbol{R}_\mathbf{H}\cdot\mathbf{c}_j^{(2)}$ + $\boldsymbol{R}_\mathbf{V}\cdot\mathbf{c}_j^{(1)}$ = 10 at PD2. After the differential detection, the detected power units are – 4 power unit, and the data bit '0' for user #6 is obtained.

An example of received power units for matched and unmatched codecs is shown as Table 3. Where user #6 is the matched codec with b_6=1, user #3 and user#4 are the un-matched codec with b_3=1 and b_8=0, which are detected at decoder #6, respectively. It is obvious that the numbers of wavelengths for unmatched are equal at PD1 and PD2.

Table 3.
Power detected for matched and un-matched codecs with specified ternary sequence.

	Received signal for user#6 (C_6^1 and C_6^2): Vertical SOP	λ_1	λ_2	λ_3	λ_4	λ_5	λ_6	λ_7	λ_8	Horizontal SOP	λ_1	λ_2	λ_3	λ_4	λ_5	λ_6	λ_7	λ_8	Detected power units
PD 1	$C_6^2 \bullet C_6^1$	0	0	0	0	0	0	0	0	$C_6^1 \bullet C_6^2$	0	0	0	0	0	0	0	0	0
	$C_3^1 \bullet C_6^1$	0	0	0	0	0	0	0	0	$C_3^2 \bullet C_6^2$	0	0	0	1	0	0	0	0	1
	$C_8^2 \bullet C_6^1$	0	0	0	0	0	0	0	0	$C_8^1 \bullet C_6^2$	0	0	0	1	0	0	0	0	1
PD 2	$C_6^1 \bullet C_6^1$	0	0	0	0	1	1	0	0	$C_6^2 \bullet C_6^2$	0	0	1	1	0	0	0	0	4
	$C_3^2 \bullet C_6^1$	0	0	0	0	0	0	0	0	$C_3^1 \bullet C_6^2$	0	0	1	0	0	0	0	0	1
	$C_8^1 \bullet C_6^1$	0	0	0	1	0	0	0	0	$C_8^2 \bullet C_6^2$	0	0	0	0	0	0	0	0	1

5. The performance evaluation of Hybrid SPC/SAC scheme

In evaluating the performance of the proposed hybrid SPC/SAC scheme, the present study adopts a similar analysis model to that applied by the conventional SAC scheme. The symbols which appear in the following discussions are defined in [7-9]. The present evaluation assumes that each light source is unpolarized and that the optical source is an ideal flat spectrum with a magnitude of $P_{sr}/\Delta\nu$, where P_{sr} is the effective power from a single source at the receiver and $\Delta\nu$ is the optical source bandwidth in Hertz.

Referring to [7, Eq. (12)], [8, Eq. (15)] and applying Eq. (4), the detected photocurrent coming from K simultaneous active users with a chip length of N per user at the j-th upper photo-detector (i.e. PD1) is written as:First, we need to evaluate the phase induced intensity noise (PIIN). The photocurrent detected at PD1 is written as

$$I_1 = \Re\int_0^\infty G_1(\nu)\,d\nu \tag{8}$$

$$= \frac{\Re P_{sr}}{N}\sum_{i=1}^{N}\sum_{k=1}^{K} b_k\left(c_k^{(1)}(i)\,c_j^{(1)}(i) + c_k^{(2)}(i)\,c_j^{(2)}(i)\right)$$

$$+ \frac{\Re P_{sr}}{N}\sum_{i=1}^{N}\sum_{k=1}^{K}\left(1-b_k\right)\left(c_k^{(2)}(i)\,c_j^{(1)}(i) + c_k^{(1)}(i)\,c_j^{(2)}(i)\right)$$

where $\Re$ denotes the responsibility of the photo-detector and $G(\nu)$ is assumed to be the single sideband power spectral density (PSD) of the received signal. $G_1(\nu)$ and $G_2(\nu)$ represent the upper and lower photo-detectors (i.e. PD1 and PD2), respectively. $\mathbf{c}_k(i)$ denotes the i-th chip of the k-th user codeword coming from the star coupler, and $c_j(i)$ acts as the desired decoder. The photocurrent detected at PD2 is written as

$$I_2 = \Re \int_0^{\infty} G_2(\nu)\, d\nu \tag{9}$$

$$= \frac{\Re P_{sr}}{N} \sum_{i=1}^{N} \sum_{k=1}^{K} (1-b_k)\left(c_k^{(1)}(i)\, c_j^{(1)}(i) + c_k^{(2)}(i)\, c_j^{(2)}(i)\right)$$

$$+ \frac{\Re P_{sr}}{N} \sum_{i=1}^{N} \sum_{k=1}^{K} b_k \left(c_k^{(2)}(i)\, c_j^{(1)}(i) + c_k^{(1)}(i)\, c_j^{(2)}(i)\right)$$

$c_k^{(1)}(i)$ and $c_k^{(2)}(i)$ are the i-th wavelength element of $c_k^{(1)}$ and $c_k^{(2)}$, respectively.

$$I_1 - I_2 = \begin{cases} \Re P_{sr}/2 & \text{for } k=j \text{ and } b_k = 1 \\ -\Re P_{sr}/2 & \text{for } k=j \text{ and } b_k = 0 \\ 0 & \text{for } k \neq j \end{cases} \tag{10}$$

Since collision wavelengths characterized with orthogonal polarization states are split two branches via PBS, the number of collision wavelengths becomes $N/8$ or 0 at each photo- detector. The variance of photo-detector current is expressed as

$$\langle i^2 \rangle \approx I^2 (1+P^2)\tau_c B \tag{11}$$

where I,, B, τ_c, and P denotes the average photocurrent; the noise-equivalent electrical bandwidth of the receiver; the coherence time of the source and the degree of polarization (DOP), respectively. Since Heismann *et. al.* [10] had developed P = 0.03 with setting up depolarizer in front of photo-detector, the degree of polarization P is negligible on Eq. (11).

The variances of the upper and lower photocurrents resulting from the PIIN are independent and can be written as:

$$\left\langle I_{\mathrm{PIIN}}^2 \right\rangle = \left\langle I_1^2 \right\rangle + \left\langle I_2^2 \right\rangle = B\Re^2 \int_0^{\infty} G_1^2(\nu) + G_2^2(\nu)\, d\nu \tag{12}$$

where B denotes the noise-equivalent electrical bandwidth of the receiver.

Referring to [7, Eq. (14)] and [8, Eq. (10)], the variance of the differential photocurrent resulting from the PIIN is then given by [see Appendix]:

$$\left\langle I_{\mathrm{PIIN}}^2 \right\rangle = \left\langle I_1^2 \right\rangle + \left\langle I_2^2 \right\rangle = B\Re^2 \int_0^{\infty} G_1^2(\nu) + G_2^2(\nu)\, d\nu$$

$$= \frac{B\Re^2 P_{sr}^2}{N\Delta\nu}\left(\frac{NK}{2} + \frac{NK(K-2)}{8}\right) \times \frac{1}{2}$$

$$= \frac{B\Re^2 P_{sr}^2}{N\Delta\nu} \times \frac{NK(K+2)}{16} \tag{13}$$

Dividing Eq. (10) by Eq. (13), The signal-to-noise ratio **(*SNR*)** and bit-error-rate, under the assumption that Gaussian approximation, is written as

$$SNR = \frac{\langle I_{b=1} - I_{b=0} \rangle^2}{B\left\langle I_{PIIN}^2 \right\rangle} = \frac{16\Delta\nu}{BK(K+2)} \tag{14}$$

where $\Delta\nu$ is optical band-width and K is number of active users. Here, the Gaussian approximation is used for the calculation of bit error rate (***BER***).

$$BER = \frac{1}{2} erfc\left(\sqrt{\frac{SNR}{8}}\right) \tag{15}$$

Compared to conventional scheme, the variable SNR is shown as Table 4.

Table 4
The $SNR_{(PIIN)}$ of hybrid SPC/SAC coding scheme (setting DO*P*=0).

Applied scheme (Walsh-Hadamard)	Constructed Matrix	Codeword Length	Weight	User Capacity	Cross-correlation (single arm) k-th and j-th codeword $R_{cc}(k,j)$	$SNR_{(PIIN)}$
Conventional unipolar SAC scheme	$N=2^m$	N	$N/2$	N-1	$N/4$	$\frac{\Delta\upsilon}{BK(K+1)}$
omplementary unipolar SAC scheme	$N=2^m$	N	$N/2$	N-1	$N/4$	$\frac{4\Delta\upsilon}{BK(K+1)}$
Previous SPC scheme (Complementary bipolar scheme)	$N=2^m$	N	N	N	$N/2$	$\frac{8\Delta\upsilon}{BK(K+1)}$
ubrid SPC/SAC scheme (Complementary bipolar scheme)	$N=2^m$	N	$N/2$	N	$N/8$	$\frac{16\Delta\upsilon}{BK(K+2)}$

while $\Delta\nu$ = 6.25 THz, and B = 1 MHz for a given error probability of 10^{-9}, the simulation results show that the number of simultaneous active users is improved 41.5% relative to the previous SPC coding scheme under DOP is set to zero for the ideal case. Also, the the number of simultaneous active users is increased 100% compared to conventional complementary SAC coding scheme and shown as Fig. 5.

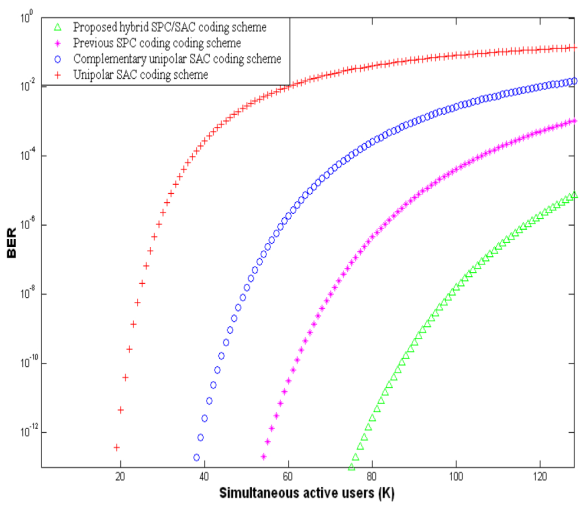

Fig. 5. Signal-to-Noise Ratio, and (b) BER vs. Simultaneous active users while $\Delta\nu$= 6.25THz, *B*=1MHz.

6. Conclusions and Discussion

The hybrid SPC/SAC created by specified orthogonal ternary matrix is presented. Compared with conventional SAC scheme, it is shown that a half of PIIN noise is reduced because that the proposed hybrid SPC/SAC scheme is characterized with less collision wavelengths at photo-detector. Furthermore, the simulation results show that the number of simultaneous active users is improved 41.5% relative to the previous SPC coding scheme under DOP is set to zero for the ideal case. Since polarization mode dispersion is minimal and can be feasible compensated in fiber transmission channel in 1~2 km distance range, the hybrid SPC/SAC is suitable for LAN. However, the DGD (differential group delay) increases in long haul network. Hence, the polarization state of the wavelength may rotate and make the orthogonal polarization states characteristic failure. Also, the bit error rate is increased and coherent crosstalk is possibly induced. That is, The DGD effect of proposed hybrid SPC/SAC will be discussed and investigated in the further work.

Appendix

This Appendix derives the variance of the differential photocurrent resulting from the PIIN by setting the degree of polarization to zero (i.e. P =0). Referring to [7, Eq. (14)] and [8, Eq. (10)], the variance of the j-th upper photocurrent (i.e. PD1) resulting from the PIIN is given by:

$$\left\langle \boldsymbol{I}_1^2 \right\rangle = \boldsymbol{B}\,\Re^2 \int_0^{\infty} \boldsymbol{G}_1^2(\nu)\,\mathrm{d}\nu$$

$$= \frac{\boldsymbol{B}\,\Re^2 P_{\mathrm{sr}}^2}{\Delta\nu} \sum_{i=1}^{\boldsymbol{N}} \left\{ \left[\sum_{k=1}^{\boldsymbol{K}} \left(\mathrm{b}_k \boldsymbol{S}_{k,j}(i) + (1-\mathrm{b}_k) \boldsymbol{D}_{k,j}(i) \right) \right] \times \left[\sum_{m=1}^{\boldsymbol{K}} \left(\mathrm{b}_m \boldsymbol{S}_{m,j}(i) + (1-\mathrm{b}_k) \boldsymbol{D}_{m,j}(i) \right) \right] \right\} \quad \text{(A1)}$$

where by definition: $\boldsymbol{S}_{k,j}(i) = \boldsymbol{c}_k^{(1)}(i)\,\boldsymbol{c}_j^{(1)} + \boldsymbol{c}_k^{(2)}(i)\,\boldsymbol{c}_j^{(2)}(i)$

$$\boldsymbol{D}_{k,j}(i) = \boldsymbol{c}_k^{(2)}(i)\,\boldsymbol{c}_j^{(1)}(i) + \boldsymbol{c}_k^{(1)}(i)\,\boldsymbol{c}_j^{(2)}(i)$$

$$\boldsymbol{S}_{m,j}(i) = \boldsymbol{c}_m^{(1)}(i)\,\boldsymbol{c}_j^{(1)}(i) + \boldsymbol{c}_m^{(2)}(i)\,\boldsymbol{c}_j^{(2)}(i)$$

$$\boldsymbol{D}_{m,j}(i) = \boldsymbol{c}_m^{(2)}(i)\,\boldsymbol{c}_j^{(1)}(i) + \boldsymbol{c}_m^{(1)}(\boldsymbol{i})\,\boldsymbol{c}_j^{(2)}(i)$$

Here, $\boldsymbol{S}_{k,j}$ indicates that the k-th user coming from the star coupler is characterized by the same state of polarization (SOP) as the j-th decoder on the upper photo-detector. Conversely, $\boldsymbol{D}_{k,j}$ indicates that the k-th user coming from the star coupler is characterized by the different state of polarization (SOP) from the j-th decoder on the upper photo-detector.

By applying the property of the proposed SPC codeword shown as follows:

$$\boldsymbol{c}_j^{(1)}(i)\,\boldsymbol{c}_j^{(1)}(i) = \boldsymbol{c}_j^{(1)}(i) \qquad \boldsymbol{c}_j^{(2)}(i)\,\boldsymbol{c}_j^{(2)}(i) = \boldsymbol{c}_j^{(2)}(i) \qquad \boldsymbol{c}_j^{(1)}(i)\,\boldsymbol{c}_j^{(2)}(i) = 0 \quad \text{(A2)}$$

and then substituting the result of Eq. (A2) into the expanded Eq. (A1) and rearranging terms, the variance of the j-th upper photocurrent (PD1) is given as:

$$\left\langle \boldsymbol{I}_1^2 \right\rangle = \frac{\boldsymbol{B}\,\Re^2 P_{\mathrm{sr}}^2}{\Delta\nu} \sum_{i=1}^{\boldsymbol{N}} \sum_{k=1}^{\boldsymbol{K}} \sum_{m=1}^{\boldsymbol{K}} \left(\mathbf{V}_{k,m}(i)\,\boldsymbol{c}_j^{(1)}(i) + \mathbf{H}_{k,m}(i)\,\boldsymbol{c}_j^{(2)}(i) \right) \quad \text{(A3)}$$

where, by definition:

$$\mathbf{V}_{k,m}(i) = \mathrm{b}_k \mathrm{b}_m \boldsymbol{c}_k^{(1)}(i)\,\boldsymbol{c}_m^{(1)}(i) + (1-\mathrm{b}_k)\mathrm{b}_m \boldsymbol{c}_k^{(2)}(i)\,\boldsymbol{c}_m^{(1)}(i) + \mathrm{b}_k(1-\mathrm{b}_m)\boldsymbol{c}_k^{(1)}(i)\,\boldsymbol{c}_m^{(2)}(i) + (1-\mathrm{b}_k)(1-\mathrm{b}_m)\boldsymbol{c}_k^{(2)}(i)\,\boldsymbol{c}_m^{(2)}(i)$$

$$\mathbf{H}_{k,m}(i) = (1-\mathrm{b}_k)(1-\mathrm{b}_m)\boldsymbol{c}_k^{(1)}(i)\,\boldsymbol{c}_m^{(1)}(i) + \mathrm{b}_k(1-\mathrm{b}_m)\boldsymbol{c}_k^{(2)}(i)\,\boldsymbol{c}_m^{(1)}(i) + (1-\mathrm{b}_k)\mathrm{b}_m \boldsymbol{c}_k^{(1)}(i)\,\boldsymbol{c}_m^{(2)}(i) + \mathrm{b}_k \mathrm{b}_m \boldsymbol{c}_k^{(2)}(i)\,\boldsymbol{c}_m^{(2)}(i)$$

Similarly, the photocurrent variance at PD 2 is written as:

$$\left\langle \boldsymbol{I}_2^2 \right\rangle = \frac{\boldsymbol{B}\,\Re^2 P_{\mathrm{sr}}^2}{\Delta\nu} \sum_{i=1}^{\boldsymbol{N}} \sum_{k=1}^{\boldsymbol{K}} \sum_{m=1}^{\boldsymbol{K}} \left(\mathbf{V}_{k,m}(i)\,\boldsymbol{c}_j^{(2)}(i) + \mathbf{H}_{k,m}(i)\,\boldsymbol{c}_j^{(1)}(i) \right) \quad \text{(A4)}$$

Hence, the variance of photocurrent at PD1 and PD2 are independent. Hence, the variance is the summation of variance at

PD1 and PD2.

$$\left\langle I_{\mathbf{PIIN}}^2\right\rangle=\left\langle I_1^2\right\rangle+\left\langle I_2^2\right\rangle=B\Re^2\int_0^\infty G_1^2(\nu)+G_2^2(\nu)\ d\nu$$
$$=\frac{B\Re^2 P_{sr}^2}{N\Delta\nu}\sum_{i=1}^{N}\sum_{k=1}^{K}\sum_{m=1}^{K}\Big[\mathrm{b}_k\mathrm{b}_m S_{k,m}+\mathrm{b}_k\left(1-\mathrm{b}_m\right)D_{k,m}\left(1-\mathrm{b}_k\right)\mathrm{b}_m D_{k,m}\left(1-\mathrm{b}_k\right)\left(1-\mathrm{b}_m\right)S_{k,m}\Big] \qquad \text{(A5)}$$

where, by definition:

$$S_{k,m}\ (i)=c_k^{(1)}(i)\ c_m^{(1)}(i)+c_k^{(2)}(i)\ c_m^{(2)}(i)$$

$$D_{k,m}(i)=c_k^{(2)}(i)\ c_m^{(1)}(i)+c_k^{(1)}(i)\ c_m^{(2)}(i)$$

Following the Eq. (10), the lower-bound approximation can be obtained

$$\sum_{i=1}^{N}\left\{\sum_{k=1}^{K}\sum_{m=1}^{K}\Big[\ c_k^1(i)\ \ c_m^1(i)+c_k^2(i)\ \ c_m^2(i)\ \Big]\right\}\Big[\ c_j^1(i)+c_j^2(i)\ \Big]=N\left\{\frac{K}{2}+\frac{K\ (K-2)}{8}\right\}\cdot\frac{1}{2}=\frac{NK(K+2)}{16} \qquad \text{(A6)}$$

References

[1] D. Zaccarin and M. Kavehrad, "An optical CDMA system based on spectral encoding of LED," *IEEE Photon. Technol. Lett.,* vol. 4, pp. 479-482, Apr. 1993.

[2] Kavehrad, M. and D. Zaccarin, "Optical Code-Division-Multiplexed Systems Based on Spectral Encoding of Noncoherent Sources," *IEEE J. Lightwave Technol*., vol. 13, no. 3, pp. 534-545, March 1995.

[3] X. Zhou, H. M. H. Shalaby, C. Lu, and T. Cheng, "Code for spectral amplitude coding optical CDMA systems," *Electron. Lett*., vol. 36, pp. 728–729, Apr. 13, 2000.

[4] Z. Wei; Shalaby, H.M.H.; Ghafouri-Shiraz, H., "Modified quadratic congruence codes for fiber Bragg-grating-based spectral-amplitude-coding optical CDMA systems," *IEEE J. Lightwave Technol.*, vol. 19, no. 9, pp. 1274-1281, Sept. 2001.

[5] J.F. Huang and C.C. Yang, "Reductions of Multiple-Access Interference in Fiber–Grating -Based Optical CDMA Network," *IEEE Trans. on Commun*., vol. 50, no. 10, pp. 1680-1687, October 2002.

[6] B. Moslehi, "Noise power spectra of optical two-beam interferometers induced by the laser phase noise," *J. Lightwave Technol*., vol. 4, no. 11, pp. 1704–1710, Nov. 1986.

[7]. Z. Wei; Shalaby, H.M.H.; Ghafouri-Shiraz, H., "Modified quadratic congruence codes for fiber Bragg-grating-based spectral-amplitude-coding optical CDMA systems," IEEE J. Lightwave Technol., vol. 19, no. 9, pp. 1274-1281, Sept. 2001.

[8] E.D.J. Smith, R.J. Baikie, and D.P. Taylor, "Performance enhancement of spectral-amplitude-coding optical CDMA using pulse-position modulation," *IEEE Trans. on Commun*, vol. 46, no. 9, pp. 1176-1185, September 1998.

[9] Yao-Tang Chang and Jen-Fa Huang, "Complementary Bipolar Spectral Polarization Coding over Fiber-Grating-Based Differential Photo-detectors," to be published in Optical Engineering.

[10] F. Heismann and K.L. Tokuda, "Polarization -independent Electro-optic Depolarizer," *Optics Lett.,* Vol. 20, No.9 pp.1008-1010, May 1995.